

# Charmed hadron production in an improved quark coalescence model

Sungtae Cho\*

*Division of Science Education, Kangwon National University, Chuncheon 24341, Korea*

Kai-Jia Sun<sup>†</sup> and Che Ming Ko<sup>‡</sup>

*Cyclotron Institute and Department of Physics and Astronomy,  
Texas A&M University, College Station, Texas 77843, USA*

Su Houng Lee<sup>§</sup>

*Department of Physics and Institute of Physics and Applied Physics, Yonsei University, Seoul 03722, Korea*

Yongseok Oh<sup>¶</sup>

*Department of Physics, Kyungpook National University, Daegu 41566, Korea and  
Asia Pacific Center for Theoretical Physics, Pohang, Gyeongbuk 37673, Korea*

(Dated: April 21, 2020)

We study the production of charmed hadrons  $D^0$  and  $\Lambda_c^+$  in relativistic heavy ion collisions using the charm quark coalescence. Besides taking into consideration of changing hadron sizes in hot dense medium, which results in an enhanced coalescence probability for charm quarks of very low transverse momenta, we also include the collective flow effect on heavier resonances, which leads to a shift of massive charmed resonances to larger transverse momenta. Including the conversion of charm quarks not undergoing coalescence to hadrons by independent fragmentation, we obtain a good description of the measured yield ratio  $\Lambda_c^+/D^0$  as a function of transverse momentum in Au + Au collisions at  $\sqrt{s_{NN}} = 200$  GeV by the STAR Collaboration at the Relativistic Heavy Ion Collider.

PACS numbers: 25.75.-q, 25.75.Dw

## I. INTRODUCTION

The main goal of relativistic heavy ion collisions, such as those being carried out at Relativistic Heavy Ion Collider (RHIC) and the Large Hadron Collider (LHC), is to explore the phase diagram of matter described by quantum chromodynamics, especially the properties of deconfined quark-gluon plasma (QGP) that could be created in these collisions, and its transition to hadronic matter [1, 2]. Although the bulk properties of the created QGP are governed by light quarks and gluons, the rare heavy charm and bottom quarks produced in ultra-relativistic heavy ion collisions are also useful probes of its properties [3–18]. Studying resulting charmed and bottom hadrons, such as the  $D$  ( $B$ ) mesons and  $\Lambda_c$  ( $\Lambda_b$ ),  $\Sigma_c$  ( $\Sigma_b$ ),  $\Xi_c$  ( $\Xi_b$ ) baryons in relativistic heavy ion collisions, has thus been a topic of great interest [19–21]. In recent experiments by the STAR Collaboration, the transverse moment spectrum of  $D^0$  mesons and also the  $\Lambda_c/D^0$  ratio from Au + Au collisions have been measured [22–25]. The experimental data from collisions at 10-80% centrality shows the ratio  $\Lambda_c^+/D^0 \simeq 0.8$ –1.1 in the transverse momentum region of  $3 < p_T < 6$  GeV,

which is a very large enhancement compared to the value predicted from the fragmentation of charm quarks or from the PYTHIA results for  $p+p$  collisions [26, 27]. Such a ratio is also much larger than the prediction for the integrated yield from the statistical hadronization model, where  $\Lambda_c^+/D^0 \simeq 0.25 - 0.3$  [28–30].

Similar enhancements of the baryon to meson ratios of hadrons consisting of light and strange quarks in relativistic heavy ion collisions compared to those from  $p + p$  collisions were previously seen in experiments at RHIC [31–34], and they were successfully explained in terms of the quark coalescence model for the production of hadrons of intermediate momenta [35–39]. Extending the quark coalescence model to charm quarks, it was shown in Refs. [40, 41] that the  $\Lambda_c^+/D^0$  ratio in relativistic heavy ion collisions is also enhanced when compared with that in  $p + p$  collisions at the same energy. An improved study using a more realistic charm quark spectrum was later carried out in Ref. [19]. The predicted ratio  $\Lambda_c^+/D^0$  at  $p_T \approx 6$  GeV from this study is found to be about 0.4, which is still a factor of 2 smaller than the measured value in the STAR experiments. Recently, it was found that this ratio could be explained by the resonance recombination model (RRM) [20] after including a large number of missing charm baryon states [42].

In the present study, we improve the work of Ref. [41] by employing a more realistic charm quark spectrum and also including in the quark coalescence model the flow effect on produced heavy particles. In the usual coalescence model, such as the one employed in Refs. [19, 41],

\*sungtae.cho@kangwon.ac.kr

<sup>†</sup>Corresponding author: kjsun@tamu.edu

<sup>‡</sup>ko@comp.tamu.edu

<sup>§</sup>suhoung@yonsei.ac.kr

<sup>¶</sup>yohphy@knu.ac.kr

the transverse momentum of a produced hadron is equal to the total momentum of coalesced quarks. As a result, hadrons of different masses formed from these quarks all have same momentum, which is in contrast to the hydrodynamical picture that hadrons of larger masses are shifted to higher transverse momentum as a result of collective flow. To include this effect, we boost a produced hadron from the center of mass of coalescing quarks, where its Wigner function is calculated to give its formation probability, back to the fireball frame using the physical mass of the hadron. In this way, the momenta of produced hadrons, particularly resonances of large masses, are increased by the effect of parton collective flow. With this improved approach as well as after including possible increase of hadron sizes in hot dense medium and the fragmentation contribution from charmed quarks not used in coalescence, we obtain a good description of the measured  $D^0$  momentum spectrum and the predicted  $\Lambda_c^+/D^0$  ratio as a function of  $p_T$  also agrees nicely with the available data from RHIC without assuming the existence of missing high mass charmed baryon resonances as in Ref. [42]. In addition, we find that the total yield ratio  $\Lambda_c^+/D^0$  is around 0.64, and the ratio  $\Lambda_c^+/D^0$  at  $p_T = 8$  GeV can be as large as 0.6, which is much larger than the predictions from previous studies reported in Refs. [19, 41].

## II. QUARK MOMENTUM SPECTRA

### A. Light quarks

For the light quark momentum spectra, we adopt an approach similar to that employed in Ref. [41] by using more realistic ones from Ref. [19]. Specifically, the longitudinal momentum distribution of light quarks is assumed to be boost invariant in the rapidity range of  $|y| \leq 0.5$ . To take into account the collective flow of quark-gluon plasma, we assume that light partons have a radial flow profile of  $\beta_T(r_T) = \beta_{\max} r_T/R$  in the transverse plane of a heavy ion collision, where  $R$  is the transverse radius of the quark-gluon plasma at hadronization proper time  $\tau$ . The transverse momentum distribution of light quarks is taken to be a thermal one at temperature  $T = 165$  MeV, that is

$$\frac{dN_{q,\bar{q}}}{d^2p_T} = \frac{g_{q,\bar{q}} \tau m_T}{(2\pi)^3} \times \int \exp\left[-\frac{\gamma_T(m_T - p_T \cdot \beta_T) \pm \mu}{T}\right] d^2r_T. \quad (1)$$

In the above,  $g_{q,\bar{q}} = 6$  are the spin-color degeneracies of quarks and antiquarks,  $\mu$  is the quark baryon chemical potential with the plus and minus signs for quarks and antiquarks, respectively,  $m_T = \sqrt{p_T^2 + m_{q,\bar{q}}^2}$  is the transverse mass with  $m_{q,\bar{q}}$  being the constituent quark and antiquark masses, which are taken to be 300 MeV and 475 MeV for light and strange quarks, respectively,

$N_u$ ( $N_{\bar{u}}$ )	$N_s$	$R$ (fm)	$\tau$ (fm/c)	$T$ (MeV)	$\beta_{\max}$	$\mu$ (MeV)
243 (224)	143	8.5	4.5	165	0.5	10

TABLE I: Up and antiup quark numbers  $N_u$  and  $N_{\bar{u}}$ , strange quark number  $N_s$ , transverse radius  $R$ , hadronization proper time  $\tau$ , temperature  $T$ , and flow velocity  $\beta_{\max}$  of QGP produced at mid-rapidity of central Au + Au collisions at  $\sqrt{s_{NN}} = 200$  GeV and 0-10% centrality. The number of down and antidown quarks are the same as those of up and antiup quarks.

and  $\gamma_T = 1/\sqrt{1 - \beta_T^2}$ . As in Refs. [35, 39], we also include the contribution from gluons in the quark-gluon plasma, which are taken to have a distribution similar to that of light quarks, by converting them to quarks and anti-quarks according to the quark flavor compositions in the quark-gluon plasma. The parameters for describing the fireball of hadronizing quark-gluon plasma and the numbers of light and strange quarks and antiquarks are summarized in Table I, and their values are very similar to those used in Ref. [19].

### B. Charm quarks

For the charm quark momentum spectrum in heavy ion collisions at RHIC, we use the one parametrized in Ref. [19], which is based on results from a transport model study of charm quark energy loss and flow. It has the form

$$\frac{dN_c}{d^2p_T} = \begin{cases} a_0 \exp[-a_1 p_T^{a_2}], & p_T \leq p_0 \\ a_0 \exp[-a_1 p_T^{a_2}] + a_3 (1 + p_T^{a_4})^{-a_5}, & p_T > p_0 \end{cases} \quad (2)$$

where  $p_0 = 1.85$  GeV and the values of the parameters  $a_i$  with  $i = 1, \dots, 5$  are given in Table II. They are slightly different from those in Ref. [19] to achieve a better description of the measured  $D^0$  spectrum at large transverse momentum. Integrating the above transverse momentum spectrum gives the total number of heavy quarks of  $dN_c/dy \simeq 2.1$  for the collisions at RHIC considered in the present study. For the charm quark mass, we use  $m_c = 1.5$  GeV in the present study.

RHIC	$a_0$	$a_1$	$a_2$	$a_3$	$a_4$	$a_5$
$p_T \leq p_0$	0.69	1.15	1.57	—	—	—
$p_T \geq p_0$	1.08	3.04	0.71	9.914	2.5	3.48

TABLE II: Parameters used in the parametrization of charm quark transverse momentum spectrum at mid-rapidity of central Au + Au collisions at  $\sqrt{s_{NN}} = 200$  GeV.

### III. QUARK COALESCENCE

For simplicity, we assume as in Ref. [41] that the spatial distribution of quarks is uniform in the thermalized QGP inside a fire cylinder of volume  $V = \pi R^2 \tau$ . Taking the Wigner function of hadrons to be Gaussian in space and in momentum and neglecting the space and velocity correlation of light quarks due to collective flow, we can integrate out the spatial part of the coalescence formula and obtain the transverse momentum spectrum of produced heavy mesons of certain species as

$$\frac{dN_M}{d\mathbf{p}_M} = g_M \frac{(2\sqrt{\pi}\sigma)^3}{V} \int d\mathbf{p}_1 d\mathbf{p}_2 \frac{dN_1}{d\mathbf{p}_1} \frac{dN_2}{d\mathbf{p}_2} \times \exp(-\mathbf{k}^2 \sigma^2) \delta(\mathbf{p}_M - \mathbf{p}_1 - \mathbf{p}_2). \quad (3)$$

In the above,  $g_M$  is the statistical factor for colored spin-1/2 quark and antiquark to form a color neutral meson, e.g.,  $g_{D^0} = 1/36$  and  $g_{D^{*0}} = 1/12$  for  $D^0$  and  $D^{*0}$ , respectively. The momenta  $\mathbf{p}_1$ ,  $\mathbf{p}_2$ , and  $\mathbf{p}_M$  are those of the heavy quark, light quark, and produced heavy meson, respectively, with the  $\delta$  function to ensure the momentum conservation. The relative transverse momentum  $\mathbf{k}$  between the heavy quark of mass  $m_1$  and light antiquark of mass  $m_2$  is defined as

$$\mathbf{k} = \frac{1}{m_1 + m_2} (m_2 \mathbf{p}'_1 - m_1 \mathbf{p}'_2), \quad (4)$$

where  $\mathbf{p}'_1$  and  $\mathbf{p}'_2$  are the momenta of the heavy quark and light antiquark in the center of mass frame of produced heavy meson. The width parameter  $\sigma$  is related to the harmonic oscillator frequency  $\omega_M$  by  $\sigma = 1/\sqrt{\mu\omega_M}$  with  $\mu = m_1 m_2 / (m_1 + m_2)$  being the reduced mass.

Similarly, the momentum spectrum of heavy baryons from the coalescence of a charm quark and two light quarks can be calculated according to

$$\frac{dN_B}{d\mathbf{p}_B} = g_B \frac{(2\sqrt{\pi})^6 (\sigma_1 \sigma_2)^3}{V^2} \int d\mathbf{p}_1 d\mathbf{p}_2 d\mathbf{p}_3 \frac{dN_1}{d\mathbf{p}_1} \frac{dN_2}{d\mathbf{p}_2} \frac{dN_3}{d\mathbf{p}_3} \times \exp(-\mathbf{k}_1^2 \sigma_1^2 - \mathbf{k}_2^2 \sigma_2^2) \delta(\mathbf{p}_B - \mathbf{p}_1 - \mathbf{p}_2 - \mathbf{p}_3), \quad (5)$$

where the index 3 refers to the heavy quark and indices 1 and 2 refer to light quarks, and  $g_B$  is the statistical factor, which, for example, is 1/108 for  $\Lambda_c$ , 1/36 for  $\Sigma_c$ , 1/54 for  $\Xi^c$  ( $\Xi_c^*$ ), and 1/8 for  $\Sigma_c^*$  and  $\Xi_c^*$ . The relative transverse momenta are defined as

$$\mathbf{k}_1 = \frac{1}{m_1 + m_2} (m_2 \mathbf{p}'_1 - m_1 \mathbf{p}'_2),$$

$$\mathbf{k}_2 = \frac{1}{m_1 + m_2 + m_3} [m_3 (\mathbf{p}'_1 + \mathbf{p}'_2) - (m_1 + m_2) \mathbf{p}'_3], \quad (6)$$

with  $\mathbf{p}'_1$ ,  $\mathbf{p}'_2$  and  $\mathbf{p}_3$  being the momenta of the heavy quark and two light quarks in the center of mass frame of produced heavy baryon. The width parameters  $\sigma_i$  are

related to the oscillator parameter  $\omega_B$  by  $\sigma_i = 1/\sqrt{\mu_i \omega_B}$  with

$$\mu_1 = \frac{m_1 m_2}{m_1 + m_2}, \quad \mu_2 = \frac{(m_1 + m_2) m_3}{m_1 + m_2 + m_3}. \quad (7)$$

As in Ref. [41], we take the oscillator constants  $\omega_M$  for  $D_0$  meson and  $\omega_B$  for  $\Lambda_c^+$  baryon as parameters, and determine their values by fitting the spectrum of  $D_0$  meson and requiring all the charm quarks at low momenta to hadronize by quark coalescence. To include the flow effect on produced hadrons, we carry out the coalescence calculation at the medium rest frame and then boosting these hadrons to the fireball frame. Because of the smaller quark thermal velocity than the flow velocity, the flow effect can be approximately included by first calculating the formation probability of a charmed hadron from coalescing charm and light quarks using its Wigner function evaluated in the center of mass of these quarks and then boosting the resulting charm hadron to the fireball frame using its physical mass. This approximation results in the multiplication of the momentum  $\mathbf{p}_M$  and  $\mathbf{p}_B$  in the delta functions in Eqs.(3) and (4) by the factor  $(E_1 + E_2)/E_M$  and  $(E_1 + E_2 + E_3)/E_B$ , respectively, where  $E_i = \sqrt{m_i^2 + \mathbf{p}_i^2}$  and  $E_{M,B} = \sqrt{m_{M,B}^2 + \mathbf{p}_{M,B}^2}$  with  $m_{M,B}$  being the mass of produced heavy hadrons. In this case, heavy resonances with large masses would have large transverse momenta in the rest frame of the expanding QGP, which is consistent with the hydrodynamic picture that the additional momenta acquired by particles due to the collective flow are larger if they are more massive. This effect has been neglected in previous studies based on the coalescence approach [19, 41] where the transverse momentum spectrum of produced particles is independent of their masses. The present approach is thus more appropriate for studying the production of massive resonances in relativistic heavy ion collisions. We note that the production of massive hadrons is not suppressed in the coalescence model as it is based on the sudden approximation. This is in contrast to that in the resonance recombination model of Ref. [20] used in Ref. [42] due to the required energy conservation in this approach.

### IV. CHARM QUARK FRAGMENTATION

Similarly to Refs. [19, 41], charm quarks that are not used for producing hadrons via coalescence with light quarks are converted to hadrons by fragmentation. In terms of the fragmentation probability  $P_{\text{frag}}(p_T) = 1 - P_{\text{coal}}(p_T)$  of a charm quark of transverse momentum  $p_T$ , where  $P_{\text{coal}}(p_T)$  is its probability to coalesce with light quarks, the momentum spectrum of certain hadron species from the fragmentation of non-coalesced charm quarks is given by

$$\frac{dN_{\text{had}}}{d^2 p_T} = \sum \int dz P_{\text{frag}}(P_T) \frac{dN_{N_c}}{d^2 p_T} \frac{D_{\text{had}/c}(z, Q^2)}{z^2}. \quad (8)$$

Meson	Mass (MeV)	$I(J)$		
$D^+ = \bar{d}c$	1869	$\frac{1}{2}(0)$		
$D^0 = \bar{u}c$	1865	$\frac{1}{2}(0)$		
$D_s^+ = \bar{s}c$	1968	$0(0)$		
Resonances			Decay modes	B.R.
$D^{*+} = \bar{d}c$	2010	$\frac{1}{2}(1)$	$D^0\pi^+$ $D^+X$	68% 32%
$D^{*0} = \bar{u}c$	2007	$\frac{1}{2}(1)$	$D^0\pi^0$ $D^0\gamma$	62% 38%
$D_s^{*+} = \bar{s}c$	2112	$0(1)$	$D_s^+X$	100%

TABLE III: Charmed mesons considered in the present study. The branching ratios (B.R.) of resonances decaying to the ground states are taken from Ref. [44].

Baryon	Mass (MeV)	$I(J)$		
$\Lambda_c^+ = udc$	2286	$0(\frac{1}{2})$		
$\Xi_c^+ = usc$	2467	$\frac{1}{2}(\frac{1}{2})$		
$\Xi_c^0 = dsc$	2470	$\frac{1}{2}(\frac{1}{2})$		
Resonances			Decay modes	B.R.
$\Sigma_c^0 = ddc$	2455	$1(\frac{1}{2})$	$\Lambda_c^+\pi^-$	100%
$\Sigma_c^+ = udc$	2455	$1(\frac{1}{2})$	$\Lambda_c^+\pi^0$	100%
$\Sigma_c^{*+} = uuc$	2455	$1(\frac{1}{2})$	$\Lambda_c^+\pi^+$	100%
$\Sigma_c^{*0} = ddc$	2520	$1(\frac{3}{2})$	$\Lambda_c^+\pi^-$	100%
$\Sigma_c^{*+} = udc$	2520	$1(\frac{3}{2})$	$\Lambda_c^+\pi^0$	100%
$\Sigma_c^{*++} = uuc$	2520	$1(\frac{3}{2})$	$\Lambda_c^+\pi^+$	100%
$\Xi_c^{*+} = usc$	2645	$\frac{1}{2}(\frac{3}{2})$	$\Xi_c^+\pi^0$	seen
$\Xi_c^{*0} = dsc$	2645	$\frac{1}{2}(\frac{3}{2})$	$\Xi_c^+\pi^-$	seen
$\Xi_c^{\prime+} = usc$	2580	$\frac{1}{2}(\frac{1}{2})$	$\Xi_c^+\gamma$	seen
$\Xi_c^{\prime0} = dsc$	2580	$\frac{1}{2}(\frac{1}{2})$	$\Xi_c^0\gamma$	seen

TABLE IV: Same as Table III but for charmed baryons.

In the above,  $z = p_{\text{had}}/p_c$  is the fraction of charm quark momentum carried by the produced hadron and  $Q^2 = (p_{\text{had}}/2z)^2$  is the momentum scale for the fragmentation process. For the fragmentation function  $D_{\text{had}/c}(z, Q^2)$ , we use the one from Ref. [43],

$$D_{\text{had}}(z) \propto 1 / \left[ z \left( 1 - \frac{1}{z} - \frac{\epsilon_c}{1-z} \right)^2 \right], \quad (9)$$

with  $\epsilon_c$  being a free parameter to fix the shape of the fragmentation function. In the present study, we choose  $\epsilon_c = 0.006$  for  $D$  mesons and  $\epsilon_c = 0.02$  for  $\Lambda_c$  baryons, which leads to the fragmentation branching ratios to  $D^0$ ,  $D^+$ ,  $D_s^+$ , and  $\Lambda_c^+$  being 0.607, 0.196, 0.121, and 0.076, respectively [41].

## V. RESULTS

As shown in Ref. [41], the contributions from resonances to the yield of ground state hadrons are important and should be taken into account. Tables III and IV summarize the charmed hadrons considered in the present study, which include the ground states and the resonance states of  $D$  mesons and  $\Lambda_c$  and  $\Xi_c$  baryons, as given by the Particle Data Group [44]. For the branching ratios of  $\Xi_c^*$  and  $\Xi_c'$  baryons decaying by strong or electromagnetic interactions to the  $\Xi_c$  baryon, which are not given in Ref. [44], they are assumed to be 100%. We note that all charmed meson and baryon resonances in Tables III and IV have their orbital wave functions in the  $L = 0$  states.

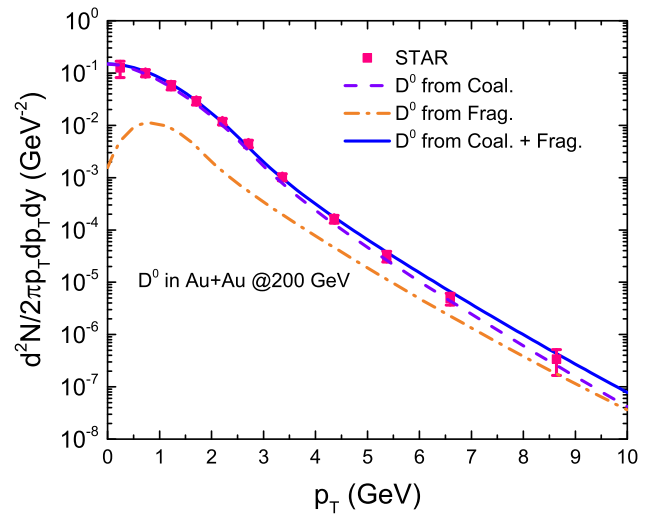


FIG. 1: Transverse momentum spectrum of  $D^0$  mesons at mid-rapidity from Au + Au collisions at  $\sqrt{s_{NN}} = 200$  GeV and (0–10%) centrality. Dashed and dash-dotted lines are the  $D^0$  spectra from charm quark coalescence and fragmentation, respectively, and their sum is given by the solid line. The experimental data shown by solid squares are taken from Ref. [45].

As in Ref. [41], we first determine the harmonic oscillator frequency  $\omega_M$  in the Wigner functions for  $D^0$ . The value of  $\omega_M \approx 0.096$  GeV is obtained from fitting the  $D^0$  transverse momentum spectrum to the data measured by the STAR Collaboration. This value is about a factor of 3 smaller than the value 0.33 GeV determined from the root-mean-square charge radius 0.43 fm of  $D^+$  as predicted by the light-front quark model [46], implying an increase of the  $D^0$  charge radius by a factor of 1.85 at temperature of 165 MeV. We note that our oscillator constant for the charmed meson is close to the value of 0.106 GeV used in Ref. [41]. Figure 1 shows our results for the  $D_0$  transverse momentum spectrum from charm quark coalescence (dashed line), fragmentation (dash-

dotted line), and their sum (solid line). It shows that the contribution from charm quark coalescence dominates at  $p_T < 10$  GeV while that of fragmentation takes over at  $p_T$  larger than around 10 GeV. This behavior is quite different from that obtained in Ref. [19] with the conventional coalescence model, which neglects the effect of flow on the momenta of produced charmed hadrons and thus results in a significant contribution from charm quark fragmentation already at  $p_T > 3$  GeV.

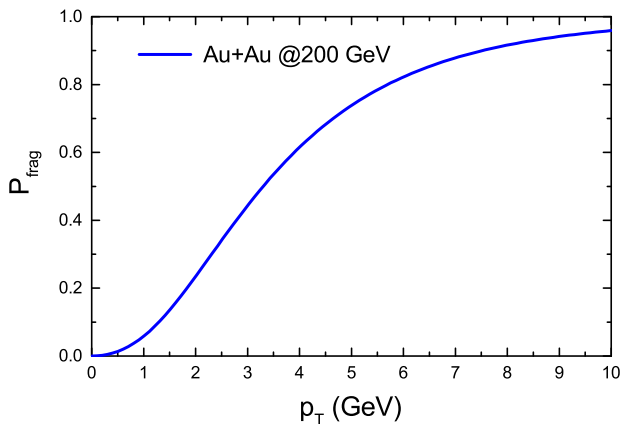


FIG. 2: Fragmentation probability of charm quarks as a function of transverse momentum for central Au+Au collisions at  $\sqrt{s_{NN}} = 200$  GeV and 0-10% centrality.

Figure 2 shows the fragmentation probability  $P_{\text{frag}}$  of charm quarks as a function of transverse momentum in central Au + Au collisions at  $\sqrt{s_{NN}} = 200$  GeV. Although charm quarks with  $p_T > 4$  GeV are more likely to hadronize by fragmentation than coalescence, only  $D_0$  mesons of  $p_T > 10$  GeV are mainly produced by charm quark fragmentation as shown in Fig. 1. This is because the charm quark in  $D^0$  from coalescence (fragmentation) mainly comes from those with momentum smaller (larger) than that of  $D^0$ .

We also compute the spectra of produced  $D_s^+$  and  $D^+$  mesons, and the results are presented in Fig. 3. It is found that although the fragmentation contribution dominates at  $p_T > 10$  GeV for  $D^+$ , which is similar to that for  $D_0$  shown in Fig. 1, it becomes important already at  $p_T > 7$  GeV for  $D_s^+$ . This is due to the softer  $D_s$  transverse momentum spectrum than that of  $D_0$  from charm quark coalescence, which is also seen in Ref. [47]. The yields of various charmed hadrons are summarized in

yield	$D^0$	$D^+$	$D_s^+$	$\Lambda_c^+$	$\Xi_c$
RHIC	0.85	0.275	0.236	0.547	0.175

TABLE V: Charmed hadron yields in central Au+Au collisions at  $\sqrt{s_{NN}} = 200$  GeV and 0-10% centrality.

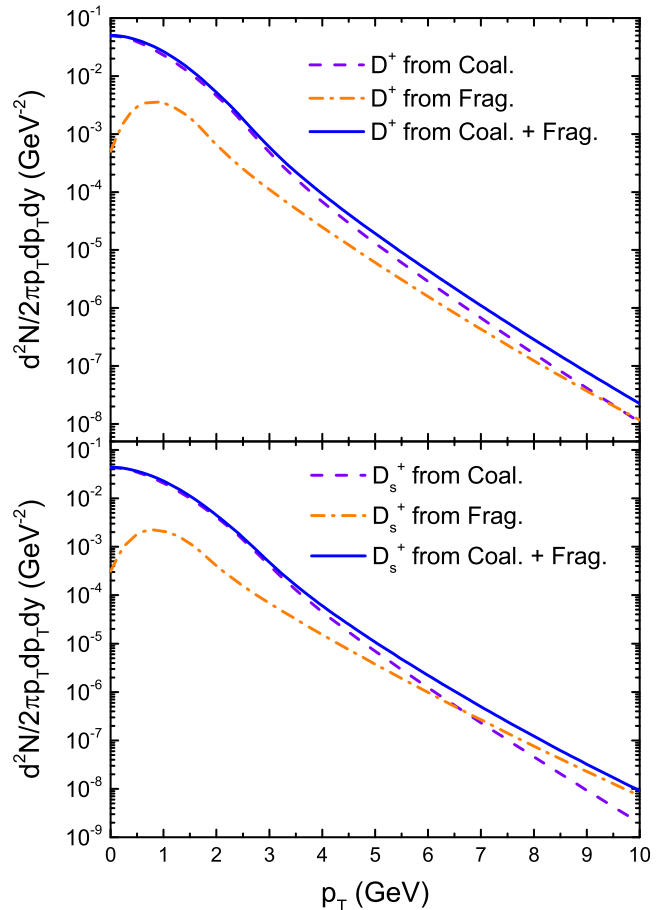


FIG. 3: Transverse momentum spectra of  $D^+$  (upper panel) and  $D_s^+$  (lower panel) mesons in central Au+Au collisions at  $\sqrt{s_{NN}} = 200$  GeV and 0-10% centrality. Dashed and dash-dotted lines are the spectra from charm quark coalescence and fragmentation, respectively, and their sum is shown by the solid line.

Table V, which shows that the total number of charmed mesons is about 1.36 with the number of  $D_0$  about three times that of  $D^+$  because of the dominant contribution from the decay of charmed meson resonances. For the remaining 0.74 charm quarks, they are converted to charmed baryons by coalescence and fragmentation as described below.

Shown in Fig. 4 is the  $\Lambda_c^+$  spectrum, which includes those from coalescence (dashed line), fragmentation (dash-dotted line), and their sum (solid line). These results are obtained with the oscillator parameter  $\omega_B = 0.16$  GeV for charmed baryons to ensure that the remaining charm quarks of very low transverse momenta, which are not used in the production of charmed mesons from the coalescence of charm quark with light antiquarks, are all used in the production of charmed baryons. This value of  $\omega_B$  corresponds to an increase of the sizes of charmed baryons at temperature of 165 MeV



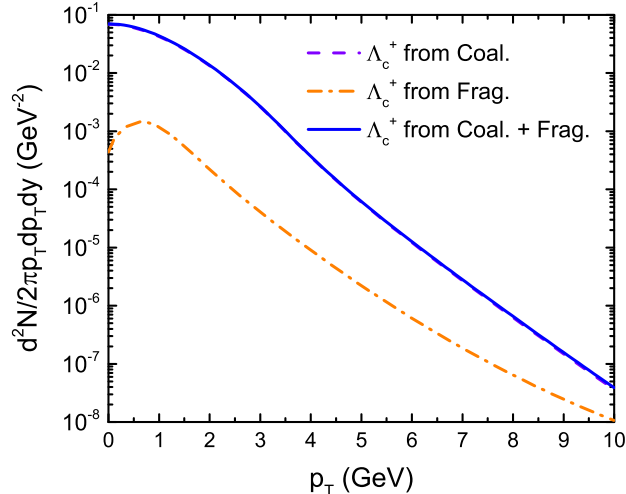


FIG. 4: Transverse momentum spectra of  $\Lambda_c^+$  baryon in Au+Au collisions at  $\sqrt{s_{NN}} = 200$  GeV and 0-10% centrality. Dashed and dash-dotted lines are the  $\Lambda_c^+$  spectra from charm quark coalescence and fragmentation, respectively, and the solid line is their sum.

compared to their values in free space using  $\omega_B = 0.33$ . This then leads to a yield of 0.547 for  $\Lambda_c^+$  and 0.175 for  $\Xi_c$  as shown in Table V. The total integrated yield ratio  $\Lambda_c^+/D_0$  is then about 0.64, which is slightly larger than the value of about 0.54 measured in  $p + p$  collisions at  $\sqrt{s} = 7$  TeV at LHC [21, 48]. We note that the oscillator constant used here for charmed baryons is larger than that for charmed mesons, which is different from that in Ref. [41] where they are taken to have the same value.

In Fig. 5, we show the yield ratio  $\Lambda_c^+/D_0$  as a function of transverse momentum in Au + Au collisions at  $\sqrt{s_{NN}} = 200$  GeV and 0-10% centrality. It is seen that the fragmentation contribution suppresses this ratio, and the results from the sum of coalescence and fragmentation contributions (dashed line) describe very well the experimental data of Ref. [25]. For  $p_T \approx 6$  GeV, the ratio  $\Lambda_c^+/D_0$  is predicted to be close to 1.0, which is much higher than the value of less than 0.4 obtained in Refs. [19, 41]. In particular, we find that the ratio  $\Lambda_c^+/D_0$  at  $p_T = 8$  GeV can be as large as 0.6, while it was predicted to be around 0.2 in Ref. [19].

Compared to the previous studies reported in Refs. [19, 41], the contribution from charm quark fragmentation in the present study is less important due to the inclusion of the flow effect on the momenta of hadrons formed from quark coalescence, which shifts higher mass charmed baryon resonances to larger transverse momenta, and this helps describe the ratio  $\Lambda_c^+/D_0$  in the transverse momentum region of  $4 < p_T < 6$  GeV.

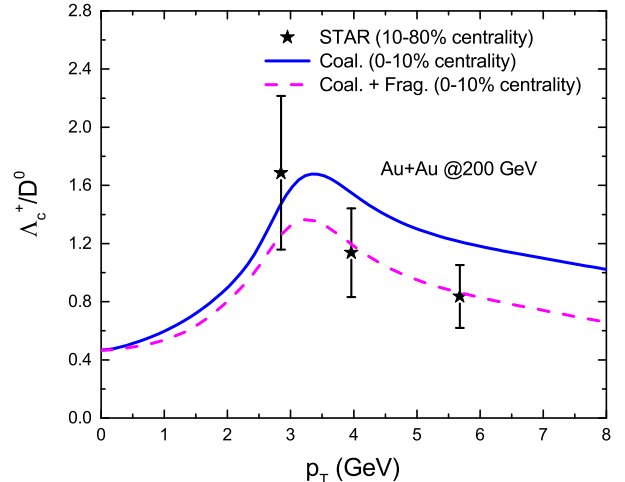


FIG. 5: The yield ratio  $\Lambda_c^+/D_0$  as a function of transverse momentum for Au + Au collisions at  $\sqrt{s_{NN}} = 200$  GeV. Solid and dashed lines denote the ratio from only charm quark coalescence and the sum of charm quark fragmentation and coalescence contributions for collisions at 0-10% centrality. The experimental data from Ref. [25] for the 10-80% centrality are shown by solid stars with combined statistical and systematic uncertainties.

## VI. CONCLUSIONS

Using the charm quark coalescence and fragmentation model with the inclusion of the effect of collective flow on the transverse momentum spectra of produced charmed hadrons, we have studied the transverse momentum spectra of charmed mesons and baryons as well as the  $\Lambda_c/D_0$  ratio. By tuning the oscillator constants in the charmed hadron Wigner functions in the quark coalescence model, which models their changing sizes in hot dense matter, to use up all the charm quarks at  $p_T \approx 0$  GeV and fragmenting the remaining charm quarks into charmed hadrons, we have obtained the ratio  $\Lambda_c^+/D_0$  as a function of  $p_T$  that successfully describes the experimental data measured at RHIC. This is in contrast to previous studies that did not include the effect of collective flow on charmed hadrons formed from quark coalescence, which underestimate substantially this ratio at  $p_T > 4.5$  GeV. Compared to results from these studies, the contribution from fragmentation is less important in the present approach. As a result, we have obtained a much larger value for  $\Lambda_c^+/D_0$  at  $p_T > 6$  GeV than that from the conventional approach. Our study thus provides an alternative description of the measured  $p_T$  dependence of the ratio  $\Lambda_c^+/D_0$  at RHIC without the inclusion of a large number of unknown charmed baryon resonances as assumed in Ref. [42]. We have, however, neglected in the present study the space-momentum correlations of both light and charm quarks, which are shown in Ref. [42] to help shift

the peak of the  $\Lambda_c^+/D^0$  ratio to higher transverse momentum. Also, the present study is based on a blast-wave model for light quarks. It is thus important to verify the validity of the results and conclusions from the present study by using the phase-space distributions of light and charm quarks from more realistic models. Since the light or strange baryon to meson ratio at  $p_T \approx 4 - 7$  GeV in the quark coalescence approach without the flow effect is very small compared to the experimentally measured value [39], it will also be very interesting to check if the inclusion of the flow effect can help resolve this discrepancy.

*Note added in proof.* After the completion of present study, similar results and conclusions have been obtained from a further improved model that uses the quark phase-space distributions from a realistic dynamic model and

also includes the production of  $p$ -wave charmed hadron resonances from quark coalescence [49].

### Acknowledgments

We are grateful to Xin Dong and Shuai Y.F. Liu for helpful discussions. This work was supported in part by the U.S. Department of Energy under Contract No. de-sc0015266, the Welch Foundation under Grant No. A-1358, and the National Research Foundation of Korea (NRF) under Grants No. NRF-2018R1D1A1B07048183, No. NRF-2018R1A6A1A06024970, No. NRF-2018R1A5A1025563, and No. NRF-2019R1A2C1087107.

- 
- [1] B. V. Jacak and B. Muller, *Science* **337**, 310 (2012).
  - [2] E. Shuryak, *Rev. Mod. Phys.* **89**, 035001 (2017).
  - [3] O. Linnyk, E. L. Bratkovskaya, and W. Cassing, *Int. J. Mod. Phys. E* **17**, 1367 (2008).
  - [4] M. He, R. J. Fries, and R. Rapp, *Phys. Rev. Lett.* **110**, 112301 (2013).
  - [5] M. He, R. J. Fries, and R. Rapp, *Phys. Rev. C* **86**, 014903 (2012).
  - [6] J. Uphoff, O. Fochler, Z. Xu, and C. Greiner, *Phys. Lett. B* **717**, 430 (2012).
  - [7] S. Cao, G.-Y. Qin, and S. A. Bass, *Phys. Rev. C* **92**, 024907 (2015).
  - [8] M. Nahrgang, J. Aichelin, S. Bass, P. B. Gossiaux, and K. Werner, *Phys. Rev. C* **91**, 014904 (2015).
  - [9] F. Scardina, S. K. Das, V. Minissale, S. Plumari, and V. Greco, *Phys. Rev. C* **96**, 044905 (2017).
  - [10] S. K. Das, M. Ruggieri, F. Scardina, S. Plumari, and V. Greco, *J. Phys. G* **44**, 095102 (2017).
  - [11] S. K. Das, S. Plumari, S. Chatterjee, J. Alam, F. Scardina, and V. Greco, *Phys. Lett. B* **768**, 260 (2017).
  - [12] S. K. Das, F. Scardina, S. Plumari, and V. Greco, *Phys. Lett. B* **747**, 260 (2015).
  - [13] S. K. Das, F. Scardina, S. Plumari, and V. Greco, *Phys. Rev. C* **90**, 044901 (2014).
  - [14] L. Tolos, J. M. Torres-Rincon, and S. K. Das, *Phys. Rev. D* **94**, 034018 (2016).
  - [15] S. Cao, T. Luo, G.-Y. Qin, and X.-N. Wang, *Phys. Rev. C* **94**, 014909 (2016).
  - [16] A. Beraudo, A. De Pace, M. Monteno, M. Nardi, and F. Prino, *JHEP* **02**, 043 (2018).
  - [17] A. Beraudo, A. De Pace, M. Monteno, M. Nardi, and F. Prino, *Eur. Phys. J. C* **75**, 121 (2015).
  - [18] W. M. Alberico, A. Beraudo, A. De Pace, A. Molinari, M. Monteno, M. Nardi, and F. Prino, *Eur. Phys. J. C* **71**, 1666 (2011).
  - [19] S. Plumari, V. Minissale, S. K. Das, G. Coci, and V. Greco, *Eur. Phys. J. C* **78**, 348 (2018).
  - [20] L. Ravagli and R. Rapp, *Phys. Lett. B* **655**, 126 (2007).
  - [21] M. He and R. Rapp, *Phys. Lett. B* **795**, 117 (2019).
  - [22] X. Dong, *Nucl. Phys.* **A967**, 192 (2017).
  - [23] G. Xie for the STAR Collaboration, *Nucl. Phys.* **A967**, 928 (2017).
  - [24] L. Zhou for the STAR Collaboration, *Nucl. Phys.* **A967**, 620 (2017).
  - [25] G. Xie on behalf of the STAR collaboration, *PoS Hard Probes 2018*, 142 (2018).
  - [26] M. Lisovskyi, A. Verbytskyi, and O. Zenaiev, *Eur. Phys. J. C* **76**, 397 (2016).
  - [27] T. Sjostrand, S. Mrenna, and P. Z. Skands, *JHEP* **05**, 026 (2006).
  - [28] I. Kuznetsova and J. Rafelski, *Eur. Phys. J. C* **51**, 113 (2007).
  - [29] A. Andronic, P. Braun-Munzinger, K. Redlich, and J. Stachel, *Phys. Lett. B* **659**, 149 (2008).
  - [30] A. Andronic, P. Braun-Munzinger, K. Redlich, and J. Stachel, *J. Phys. G* **37**, 094014 (2010).
  - [31] G. Agakishiev *et al.* (STAR Collaboration), *Phys. Rev. Lett.* **108**, 072302 (2012).
  - [32] G. Agakishiev *et al.* (STAR Collaboration), *Phys. Rev. Lett.* **108**, 072301 (2012).
  - [33] B. B. Abelev *et al.* (ALICE Collaboration), *Phys. Rev. Lett.* **111**, 222301 (2013).
  - [34] B. B. Abelev *et al.* (ALICE Collaboration), *Phys. Lett. B* **736**, 196 (2014).
  - [35] V. Greco, C. M. Ko, and P. Levai, *Phys. Rev. Lett.* **90**, 202302 (2003).
  - [36] R. J. Fries, B. Muller, C. Nonaka, and S. A. Bass, *Phys. Rev. Lett.* **90**, 202303 (2003).
  - [37] V. Greco, C. M. Ko, and P. Levai, *Phys. Rev. C* **68**, 034904 (2003).
  - [38] R. J. Fries, V. Greco, and P. Sorensen, *Ann. Rev. Nucl. Part. Sci.* **58**, 177 (2008).
  - [39] V. Minissale, F. Scardina, and V. Greco, *Phys. Rev. C* **92**, 054904 (2015).
  - [40] S. H. Lee, K. Ohnishi, S. Yasui, I.-K. Yoo, and C.-M. Ko, *Phys. Rev. Lett.* **100**, 222301 (2008).
  - [41] Y. Oh, C. M. Ko, S. H. Lee, and S. Yasui, *Phys. Rev. C* **79**, 044905 (2009).
  - [42] M. He and R. Rapp, *Phys. Rev. Lett.* **124**, 042301 (2020).
  - [43] C. Peterson, D. Schlatter, I. Schmitt, and P. M. Zerwas, *Phys. Rev. D* **27**, 105 (1983).
  - [44] K. A. Olive *et al.* (Particle Data Group), *Chin. Phys.* **C38**, 090001 (2014).
  - [45] J. Adam *et al.* (STAR Collaboration), *Phys. Rev. C* **99**,

- 034908 (2019).
- [46] C.-W. Hwang, Eur. Phys. J. C 23, 585 (2002).
- [47] J. Zhao, S. Shi, N. Xu, and P. Zhuang, **EPJ Web Conf.** **202**, 06004 (2019).
- [48] S. Acharya *et al.* (ALICE Collaboration), JHEP **04**, 108 (2018).
- [49] S. Cao, K. J. Sun, S. Y. F. Liu, W. J. Xing, G. Y. Qin, and C. M. Ko, arXiv:1911.00456 [nucl-th].